Simulations of Kinetic Electrostatic Electron Nonlinear (KEEN) Waves with Variable Velocity Resolution Grids and High-Order Time-Splitting

M. Mehrenberger

Max-Planck IPP, Garching and IRMA, Université de Strasbourg

Luminy, July 2014

Joint work : B. Afeyan, F. Casas, N. Crouseilles, A. Dodhy, E. Faou, M. Mehrenberger, E. Sonnendrücker, submitted to EPJD, special issue for the Vlasovia Conference 2013.

A short introduction to the Physics of KEEN waves

- KEEN waves are asymptotic states in Vlasov plasmas
  - non-stationary
  - non linear
  - self-organized
- Driven by a ponderomotive force generated by 2 crossing laser beams. Perturb a range in velocity depending on :
  - the amplitude of the drive
  - the duration of the drive

$\Rightarrow$ We want here to study weakly driven cases

The equations to solve

Periodic $1D \times 1D$ Vlasov-Poisson equation

$$\partial_t f + v\partial_x f + (E - E_{\mathrm{Pond}})\partial_v f = 0,\ \partial_x E = \rho(t,x) - 1,\ \rho(t,x) = \int_{\mathbb{R}} f dv.$$

Here $E_{\mathrm{Pond}}(t,x)$ is of the form

$$E_{\mathrm{Pond}}(x,t) = a_{\mathrm{Dr}}\, k_{\mathrm{Dr}}\, a(t)\, \sin(k_{\mathrm{Dr}}\, x - \omega_{\mathrm{Dr}}\, t),$$

with

$$a(t) = \frac{g(t) - g(t_0)}{1 - g(t_0)},$$

$$g(t) = 0.5(\tanh(\frac{t - t_L}{t_{wL}}) - \tanh(\frac{t - t_R}{t_{wR}})),$$

$t_0 = 0,\ t_L = 69,\ t_{wL} = t_{wR} = 20,\ t_R = 207 + \mathbf{T}_{\mathrm{Dr}},\ k_{\mathrm{Dr}} = 0.26,$ $\omega_{\mathrm{Dr}} = 0.37$. The initial condition is

$$f_0(x,v) = \frac{1}{\sqrt{2\pi}} \exp\left(-\frac{v^2}{2}\right), \quad (x,v) \in [0, 2\pi/k] \times [-6, 6].$$

Outline

- CEMRACS'2012 : VOG project
- Non uniform cubic splines
- High order splitting
- Numerical results
  - L^2 norm
  - ρ-harmonics
- Towards physical results
  - RMS quantities
  - δ-f distribution function
- Conclusion/perspectives

KEEN wave simulation on uniform grid

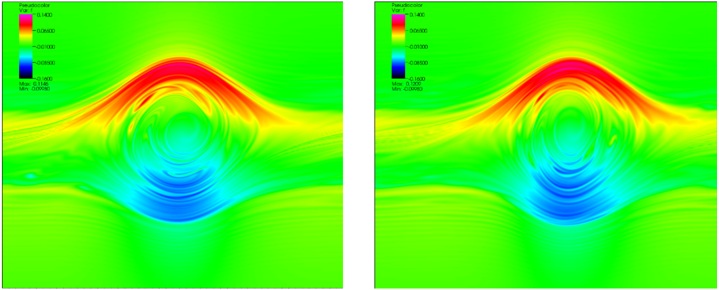

FIGURE: $f(1000, x, v) - f_0(x, v),\ \Delta t = 0.05$. Cubic splines, with $N_x = N_v = 4096$ on CPU (left) and Lagrange interpolation of degree 17 $N_x = N_v = 2048$ on GPU double precision (right).

Canonical drive $a_{\rm Dr} = 0.2,\ T_{\rm Dr} = 100.$

How to change the uniform grid ?

- Two-grid
- Non-uniform grid
- Fully adaptative

First simple strategy : non-uniform cubic splines on a two-grid mesh
Other alternatives :

- history of adaptive schemes in CALVI INRIA project
- some more recent contributions
  - real two-grid method/sparse grid (Crouseilles, M.M., Sonnendrücker, Kormann...)
  - velocity discretization (Helluy, Navoret, Pham...)
  - discontinuous Garlerkin (Madaule-Restelli, Qiu et al ; Steiner...)
  - forward PIC (Campos-Pinto ; Larson & Young)

Difficulties of **efficient** adaptive schemes
Need to measure the efficiency of the implementation

- common for PIC codes
- still not so familiar for grid based codes

A measure of the efficiency

Number of advected points in double precision in 1d per μ-second, per processor. We need

- The number of points in x N_x
- The number of points in v N_v
- The time step Δt and final time T
- The number of sub-steps s per time step (2 or 3 for Strang splitting)
- The time t of the simulation in seconds
- The number of processors n_{proc}

Formula is

$$E = \frac{N_x \cdot N_v \cdot T/\Delta t \cdot s}{10^6 \cdot t \cdot n_{\mathrm{proc}}}$$

Some examples of efficiency

Size	Sequential	GPU
256×256	29	73
2048×2048	15	414

In our code (simulation in Selalib), efficiency is around 4*, grids until* 2^{29} *points ; 256 processors are generally used but up to 2048 ; parallelization is mixed MPI/OPENMP*

- Still room for improvements !
- GPU no more competitive, using 128 or more processors.
- PIC ($2D \times 2D$) in Selalib : 13 points advected per μ-second (30 using linear splines) [Communicated by S. Hirstoaga]
- PIC up to $10^{12} \simeq 2^{40}$ points [see. S. Collombi talk]

A simple mesh with a refined zone

$$\Delta v_{\mathrm{coarse}} = \frac{v_{\max} - v_{\min}}{N_{\mathrm{coarse}}}, \ \Delta v_{\mathrm{fine}} = \frac{v_{\max} - v_{\min}}{N_{\mathrm{fine}}}$$

N_{fine} is an integer multiple of N_{coarse}.
The refined zone is chosen with $0 \leq i_1 < i_2 \leq N_{\mathrm{coarse}}$ and the total number of cells is

$$N = i_1 + N_f + N_{\mathrm{coarse}} - i_2, \ N_f = \frac{N_{\mathrm{fine}}}{N_{\mathrm{coarse}}}(i_2 - i_1)$$

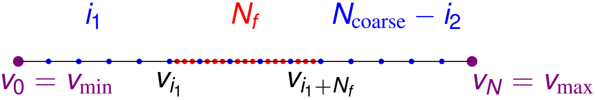

Mesh under consideration

- Canonical drive ($a_{\mathrm{Dr}} = 0.2$) : $1/6$ of velocity range

$$v_{i_1} \simeq 0.375, \; v_{i_2} \simeq 2.25$$

- Weak drive ($a_{\mathrm{Dr}} = 0.00625$) : $1/30$ of velocity range

$$v_{i_1} \simeq 1.2, \; v_{i_2} \simeq 1.6$$

We have fixed the ratio

$$\frac{N_{\mathrm{fine}}}{N_{\mathrm{coarse}}} = \frac{\Delta v_{\mathrm{coarse}}}{\Delta v_{\mathrm{fine}}} = 32.$$

Method still parametrized by the **total** *number of points* $N = N_v$

Interpolation on the mesh

- Thanks to dimensional splitting, we have to solve the 1d constant advection
$$\partial_t u + c\partial_v u = 0$$
- Use of cubic splines on non uniform mesh
- Conservative form
$$\int_{v_j}^{v_{j+1}} u(v,\Delta t)dv = \int_{v_j - c\Delta t}^{v_{j+1}-c\Delta t} u(v,0)dv.$$
  - Unknowns are in the **middle** of the velocity cells
  - Cubic splines interpolation for the primitive
  - Remove/add total mass to deal with primitive that is periodic

Note : Lagrange of degree 17 is used for advection in x. (see Charles-Després-M, SINUM 2013)

Strang splitting

Transport in x over $\Delta t/2$

$$\partial_t f(t,x,v) + v\partial_x f(t,x,v) = 0,\ t \to t + \frac{\Delta t}{2}$$

Update of E through the Poisson equation
Transport in v over Δt

$$\partial_t f(t,x,v) + E(t,x)\partial_v f(t,x,v) = 0$$

Transport in x over $\Delta t/2$

$$\partial_t f(t,x,v) + v\partial_x f(t,x,v) = 0,\ t \to t + \frac{\Delta t}{2}$$

Splitting is parametrized by
$s = 3, \sigma_{\text{init}} = 1,\ a_1 = 1/2,\ a_2 = 1,\ a_3 = 1/2.$

6-th order time splitting

$s = 11$,

$$
\begin{aligned}
a_1 = & \; 0.049086460976116245491441\,2 \\
& -2\Delta t^2(0.000069728715055305084099\,9), \\
a_2 = & \; 0.16873595056343742244819\,57, \\
a_3 = & \; 0.26417760988897670020014\,62 \\
& -2\Delta t^2(0.00062570482743004718916\,9) \\
& +4\Delta t^4(-2.91660045768984781644 \cdot 10^{-6}), \\
a_4 = & \; 0.37785158922092830388076\,6, \\
a_5 = & \; 0.18673592913490705430841\,26 \\
& -2\Delta t^2(0.0022130851240453255616\,3) \\
& +4\Delta t^4(0.0000304848026170003878868) \\
& -8\Delta t^6(4.98554938787506812159 \cdot 10^{-7}), \\
a_6 = & \; -0.0931750795687314526579244,
\end{aligned}
$$

together with $a_{6+i} = a_{6-i},\; i = 1, \ldots, 5$ and $\sigma_{\text{init}} = 0$.

History of time splitting

- Strang : second order
- Yoshida : classical triple jump
- Blanes & Moan : optimized coefficients
- For an updated litterature, see Y. Güclü et al. JCP 270 (2014), p716.
  - Strang by far the most popular
  - High order splitting is nice when combined with high order phase-space discretization with fine mesh
  - Reducing the number of stages/ size of negative coefficients is mandatory
- Here : new optimized coefficients for Vlasov-Poisson

How to find the coefficients ? Use of abstract form

- Hamiltonian is defined as $H(f) = T(f) + U(f)$, with

$$H(f) = \int_{(0,2\pi)\times\mathbb{R}} \frac{|v|^2}{2} f(x,v)dxdv + \int_{(0,2\pi)} \frac{1}{2}|E(f)(x)|^2 dx.$$

- Vlasov-Poisson can be written as

$$\partial_t f - \{\frac{\delta H}{\delta f}(f), f\} = 0,$$

with Poisson bracket $\{f,g\} = \partial_x f \cdot \partial_v g - \partial_v f \cdot \partial_x g$

- Equivalent to

$$\forall\, G, \quad \frac{\mathrm{d}}{\mathrm{dt}} G(f) = [H,G](f)$$

with Poisson bracket for functionals

$$[H,G] = \int_{(0,2\pi)\times\mathbb{R}} \frac{\delta H}{\delta f}(f)\{\frac{\delta G}{\delta f}(f), f\}\mathrm{d}x\mathrm{d}v = -[G,H].$$

Relation between T and U

- We have the relation (in $1D \times 1D$)

$$[[T, U], U] = 2U$$

- This implies RKN condition

$$[[[T, U], U], U] = 0.$$

Derivation of high order methods

- We write

$$\psi_p^\tau = e^{b_1\tau U}\, e^{a_1\tau T}\, e^{b_2\tau U} \cdots e^{b_2\tau U}\, e^{a_1\tau T}\, e^{b_1\tau U}$$

- Using for example the Baker-Campbell-Haussdorff formula, we get

$$\psi_p^\tau = e^{\tau(T+U)+R(\tau)}$$

where

$$\begin{aligned} R(\tau) \;=\;& \tau^2 p_{21}[T,U] + \tau^3(p_{31}[[T,U],T] + p_{32}[[T,U],U]) + \\ & \tau^4(p_{41}[[[T,U],T],T] + p_{42}[[[T,U],U],T] \\ & + p_{43}[[[T,U],U],U]) + \mathcal{O}(\tau^5) \end{aligned}$$

p_{ij} are polynomials in the parameters a_i, b_i.

Use of modified potentials

- We can incorporate the flow associated to $[[T, U], U]$.

$$\psi_p^\tau = e^{b_1\tau U + c_1\tau^3[[T,U],U]}\, e^{a_1\tau T} \ldots e^{a_1\tau T}\, e^{b_1\tau U + c_1\tau^3[[T,U],U]}$$

$\Rightarrow$ Achievement of given order with less stages

- further reduction of $e^{\tau C_i}$, when $[[T, U], U] = 2U$, with

$$\begin{aligned} C_i &= b_i U + c_i\tau^2[[T, U], U] + d_i\tau^4 W_{5,1} + e_i\tau^6 W_{7,1} \\ &= (b_i + 2c_i\tau^2 + 4d_i\tau^4 - 8e_i\tau^6)U \end{aligned}$$

with

$$\begin{aligned} W_{5,1} &= [U, [U, [T, [T, U]]]] \\ W_{7,1} &= [U, [T, [U, [U, [T, [T, U]]]]]]. \end{aligned}$$

L_2 norm

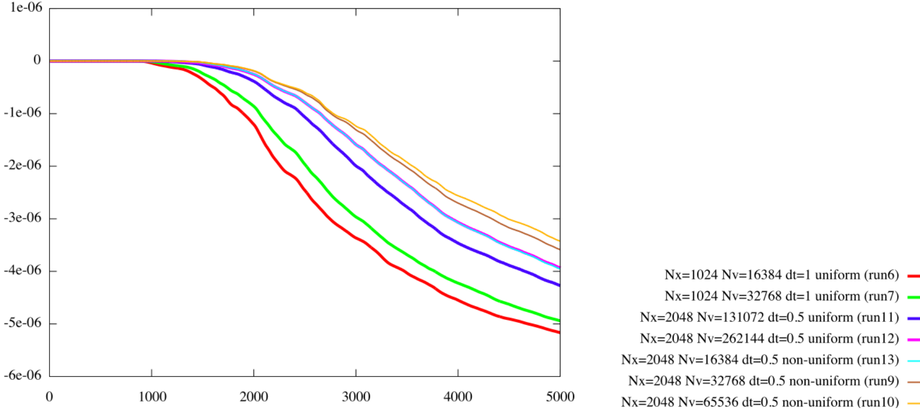

FIGURE: Time evolution of relative L_2-norm for the **small drive** amplitude case for different runs, with uniform and non-uniform velocity mesh. The 6-th order time splitting scheme is used for all the runs.

L_2 norm

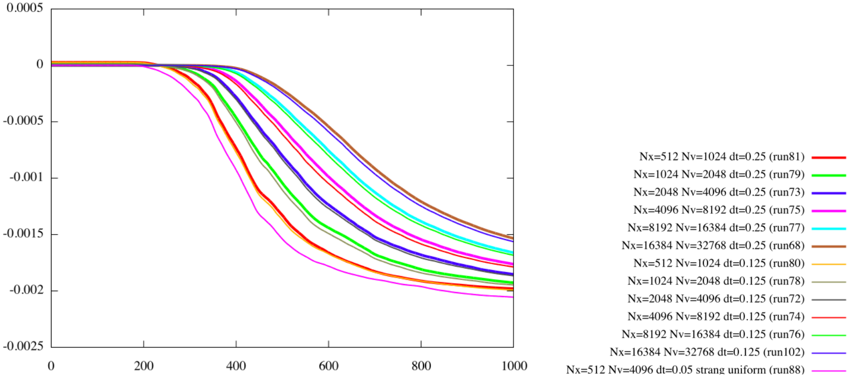

FIGURE: Time evolution of relative L_2-norm for the canonical drive amplitude case, with non-uniform velocity grids, 6-th order time splitting and different phase-space resolutions and time steps ; only the last plot uses Strang splitting and uniform velocity grid.

L_2 norm

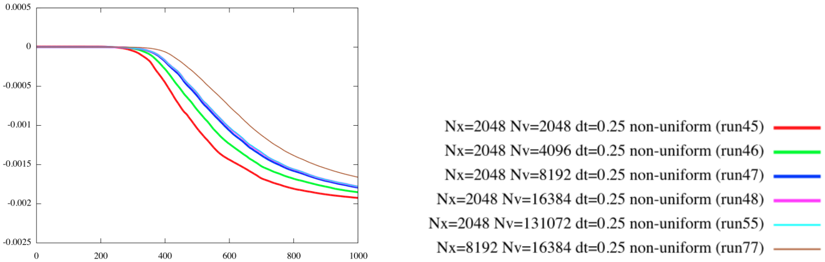

FIGURE: Time evolution of relative L_2-norm for the canonical drive amplitude case : comparison of non-uniform runs with different velocity resolution and **space resolution** $N_x = 2048$, and with canonical non-uniform run, using $N_x = 8192$. Here $\Delta t = 0.25$.

L_2 norm

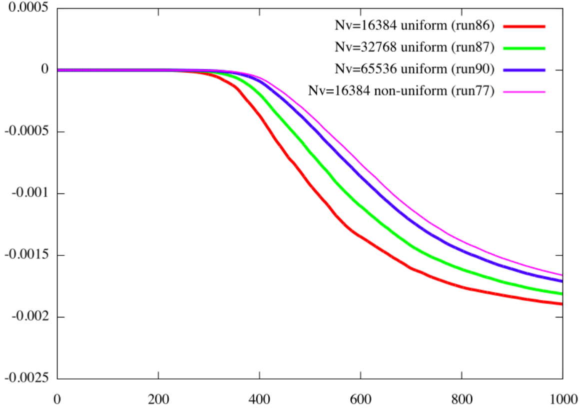

FIGURE: Time evolution of relative L_2-norm for the canonical drive case : comparison of **uniform** grid runs with different velocity resolution and a canonical non-uniform velocity grid run. Here $N_x = 8192$ throughout.

L_2 norm

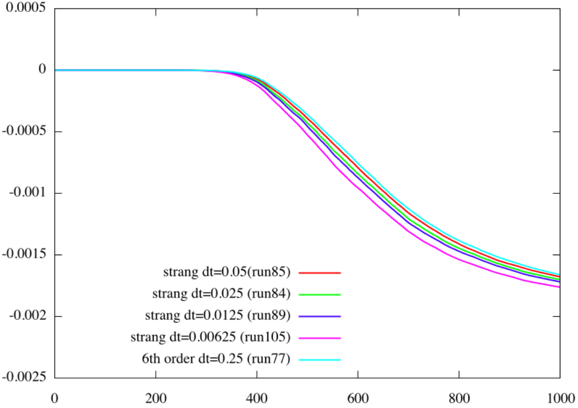

FIGURE: Time evolution of relative L_2-norm for the canonical drive amplitude case : comparison of non-uniform runs with **Strang** splitting and different time steps ; and also with canonical non-uniform run with 6th order scheme. Here $N_x = 8192, \ N_v = 16384$.

L_2 norm

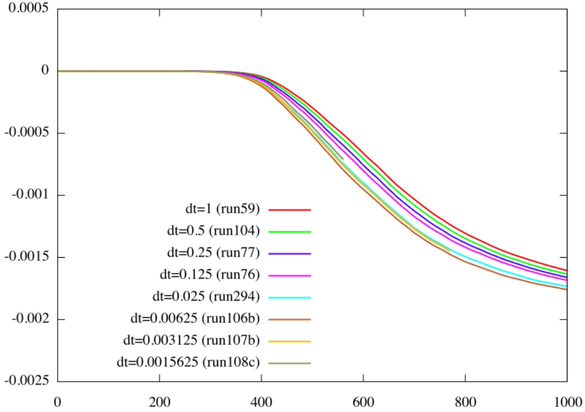

FIGURE: Time evolution of relative L_2-norm for the canonical drive amplitude case : comparison of non-uniform runs with 6**th order** scheme and different time steps. Here $N_x = 8192, \; N_v = 16384$.

L_2 norm

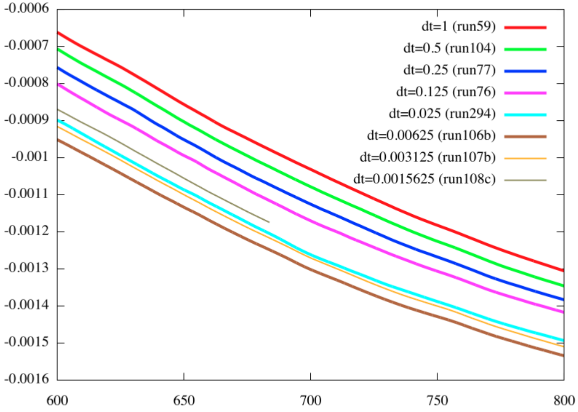

FIGURE: Zoom of previous picture for $t \in [600, 800]$.

Comparisons for the small drive

- default scheme : non-uniform cubic splines with 6-th order time splitting
- $N_v = 262144$ (uniform) comparable to $N_v = 16384$ (top-left)
- $\Delta t = 0.0078125$ (Strang) comparable to $\Delta t = 0.5$ (bottom-left)
- $N_v = 16384$ comparable to $N_v = 65536$ (top-right)
- $\Delta t = 0.5$ comparable to $\Delta t = 0.25$ (bottom-right)

Comparisons on the ρ-harmonics (small drive)

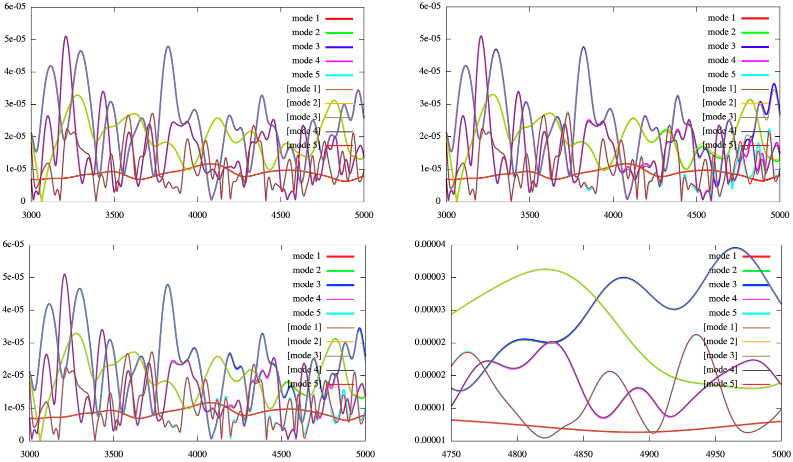

FIGURE: Comparison of the time evolution of the first 5 ρ harmonics, in the **small drive** amplitude case.

Comparisons for the canonical drive

- default scheme : non-uniform cubic splines with 6-th order time splitting
- $N_v = 65536$ (uniform) comparable to $N_v = 16384$ (top-left)
- $\Delta t = 0.0125$ (Strang) comparable to $\Delta t = 0.25$ (bottom-left)
- $(N_x, N_v) = (8192, 16384)$ comparable to $(N_x, N_v) = (16384, 32768)$ (top-right)
- $\Delta t = 0.25$ comparable to $\Delta t = 0.125$ (bottom-right)

Comparisons on the ρ-harmonics (canonical drive)

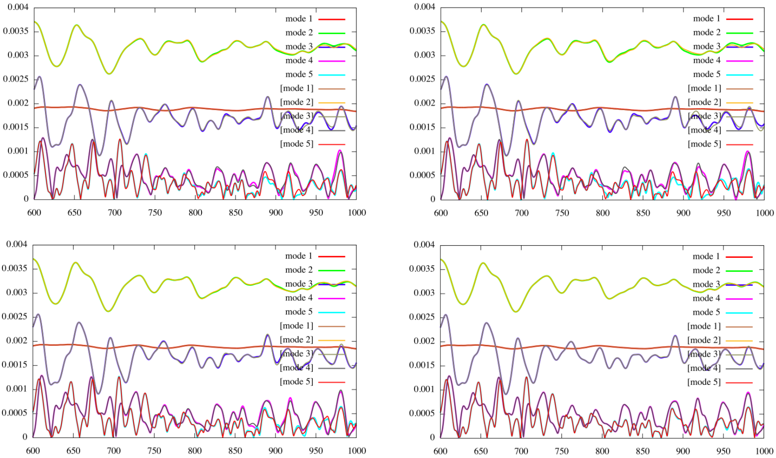

FIGURE: Comparison of the time evolution of the first 5 ρ harmonics, in the **canonical drive** case

Study of KEEN waves formation

- Other diagnostics
  - RMS quantity $\sqrt{\int_{\mathbb{R}} |\hat{f}^{(k)}(t,v)|^2 dv}$
  - δ-f distribution function
- Link with KEEN waves formation
  - consider weak drive $a_{\mathrm{Dr}} = 0.00625$
  - change the duration of the drive : $T_{\mathrm{Dr}} \in \{100, 150, 200\}$

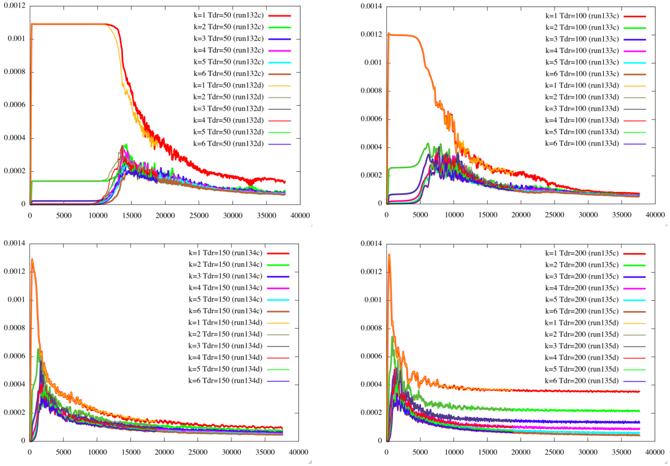

FIGURE: Time evolution of $\sqrt{\int_{\mathbb{R}} |\hat{f}^{(k)}(t,v)|^2 dv}$ for $k = 1,\ 2, \dots, 6$ and for drive time $50,\ 100,\ 150,\ 200$ (run132c-135c and run132d-135d) Parameters are $N_x = 4096,\ N_v = 32768$, non-uniform, 6-th order time scheme and $\Delta t = \mathbf{0.5}$ for run132c-135c, $\Delta t = \mathbf{0.25}$ for run132d-135d.

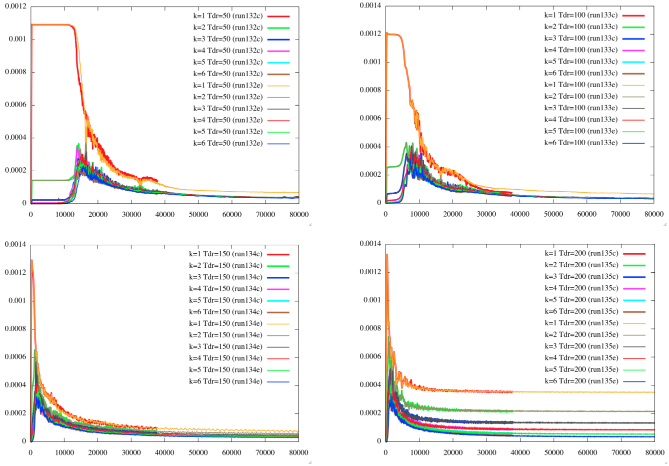

FIGURE: Time evolution of $\sqrt{\int_{\mathbb{R}} |\hat{f}^{(k)}(t,v)|^2 dv}$ for $k = 1,\ 2, \ldots, 6$ and for drive time $50,\ 100,\ 150,\ 200$ (run132c-135c and run132e-135e) Parameters are $\Delta t = 0.5$, non-uniform, 6-th order time scheme and $(N_x, N_v) = (\mathbf{4096}, \mathbf{32768})$ for run132c-135c, $(N_x, N_v) = (\mathbf{2048}, \mathbf{16384})$ for run132e-135e.

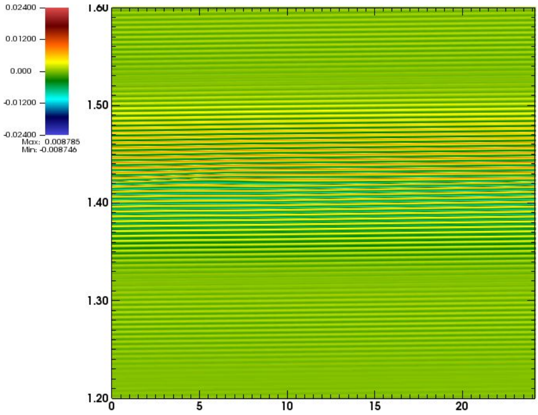

FIGURE: Case $a_{\mathrm{Dr}} = 0.00625$ and $T_{\mathrm{Dr}} = \mathbf{100}$. δf distribution function $f - f_0$ at time $T = 5000$ as a function of $(x, v) \in [0, 4\pi] \times [1.2, 1.6]$ (from top to bottom) Parameters are $N_x = 2048,\ N_v = 16384,\ \Delta t = 0.5$ non-uniform, 6-th order time scheme (run13).

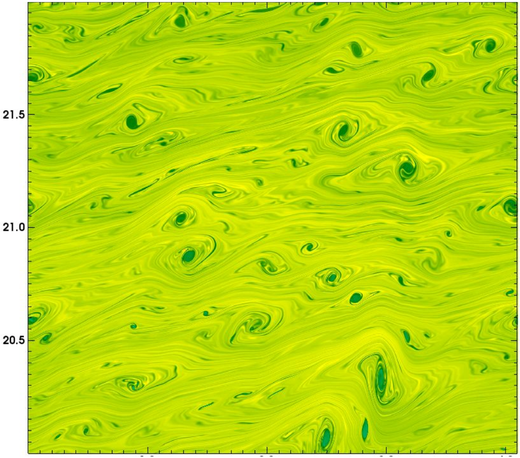

FIGURE: Details (1/3) of δf distribution function $(f - f_0)(x_i, v_j)$ at time $T = 36000$ as a function of $(i, j) \in [0, N_x] \times [16000, 22000]$ Parameters are $N_x = 4096$, $N_v = 32768$, $\Delta t = 0.5$, non-uniform, 6-th order time scheme, $T_{\rm Dr} = \mathbf{100}$, $a_{\rm Dr} = 0.00625$ (run133c).

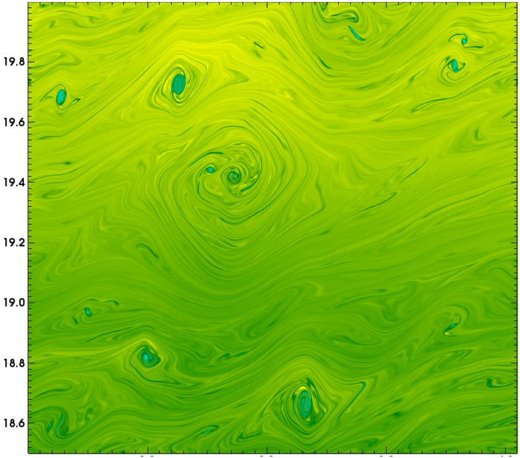

FIGURE: Details (2/3) of δf distribution function $(f - f_0)(x_i, v_j)$ at time $T = 36000$ as a function of $(i, j) \in [0, N_x] \times [16000, 22000]$ Parameters are $N_x = 4096$, $N_v = 32768$, $\Delta t = 0.5$, non-uniform, 6-th order time scheme, $T_{\rm Dr} = \mathbf{100}$, $a_{\rm Dr} = 0.00625$ (run133c).

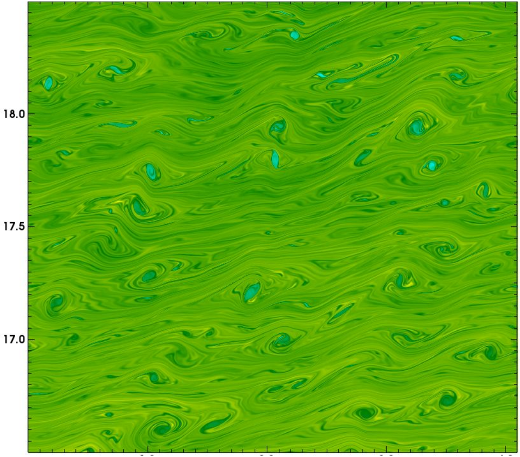

FIGURE: Details (3/3) of δf distribution function $(f - f_0)(x_i, v_j)$ at time $T = 36000$ as a function of $(i, j) \in [0, N_x] \times [16000, 22000]$ Parameters are $N_x = 4096$, $N_v = 32768$, $\Delta t = 0.5$, non-uniform, 6-th order time scheme, $T_{\mathrm{Dr}} = \mathbf{100}$, $a_{\mathrm{Dr}} = 0.00625$ (run133c).

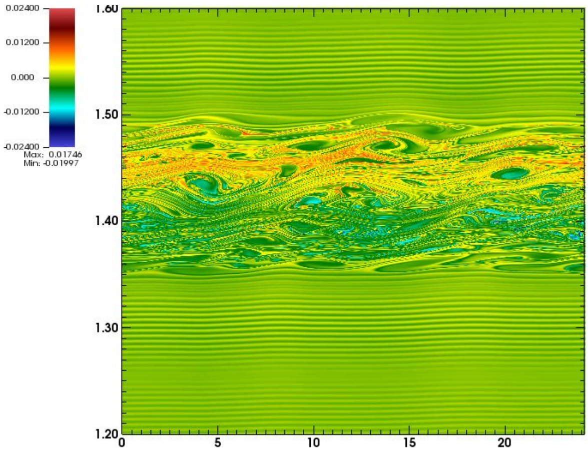

FIGURE: $a_{\mathrm{dr}} = 0.00625$ and $T_{\mathrm{dr}} = \mathbf{150}$ Parameters are
$N_x = 2048,\ N_v = 16384,\ \Delta t = 0.5$ non-uniform, 6-th order time scheme.

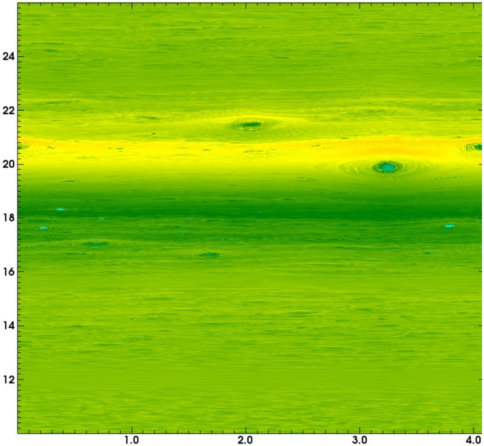

FIGURE: δf distribution function $(f - f_0)(x_i, v_j)$ at time $T = 36000$ as a function of $(i, j) \in [0, N_x] \times [13000, 26000]$. Parameters are $N_x = 4096$, $N_v = 32768$, $\Delta t = 0.5$, non-uniform, 6-th order time scheme, $T_{\mathrm{Dr}} = \mathbf{150}$, $a_{\mathrm{Dr}} = 0.00625$ (run134c).

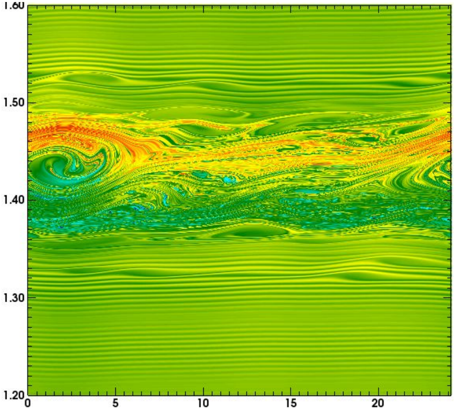

FIGURE: δf distribution function $f - f_0$ at time $T = 5000$ as a function of $(x, v) \in [0, 4\pi] \times [1.2, 1.6]$ $T_{\mathrm{Dr}} = \mathbf{200}$, $a_{\mathrm{Dr}} = 0.00625$: run with 6th order time scheme and non-uniform velocity mesh. Parameters are $N_x = 2048$, $N_v = 16384$, $\Delta t = 0.5$ non-uniform, 6-th order time scheme (run13).

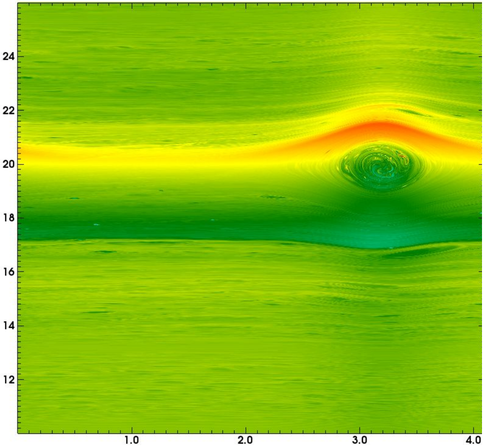

FIGURE: δf distribution function $(f - f_0)(x_i, v_j)$ at time $T = 36000$ as a function of $(i, j) \in [0, N_x] \times [13000, 26000]$. Parameters are $N_x = 4096$, $N_v = 32768$, $\Delta t = 0.5$, non-uniform, 6-th order time scheme, $T_{\mathrm{Dr}} = \mathbf{200}$, $a_{\mathrm{Dr}} = 0.00625$ (run135c).

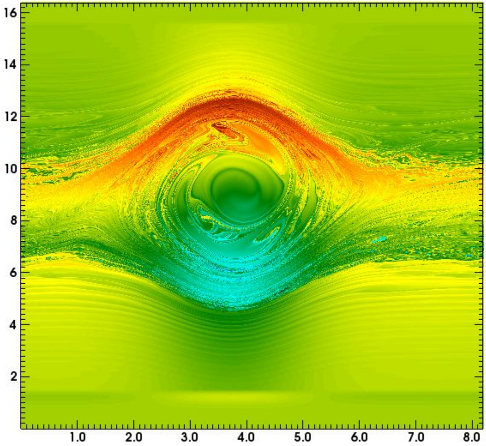

FIGURE: δf distribution function $(f - f_0)(x_i, v_j)$ at time $T = 1000$ as a function of $(i, j) \in [0, N_x] \times [0, N_v]$, in the **canonical drive** case : canonical run with 6th order time scheme and non-uniform velocity mesh. Parameters are $N_x = 8192,\ N_v = 16384,\ \Delta t = 0.25$ non-uniform, 6-th order time scheme (run77).

Conclusion

- Numerical simulation of KEEN waves with weak drive and different duration
- Study of convergence and long time behavior
- Proliferation of tiny vortices which have not coalesced vs well formed KEEN wave
- rms diagnostic helps to distinguish
- development of new numerical methods relevant for such test problem

Possible perspectives

- $4D$ simulations
- Variations of physics parameters and diagnostics
- Comparisons of numerical methods
  - discontinuous Galerkin (classical/semi-Lagrangian)
  - PIC
- Error computations, restart strategies, enhanced movie generation
- Improve performance ; multi-GPU/MIC
- How to choose the numerical parameters ?
- Convergence vs right long term averaged quantities

Some references

B. Afeyan, K. Won, V. Savchenko, T. Johnston, A. Ghizzo, and P. Bertrand, *Kinetic Electrostatic Electron Nonlinear (KEEN) waves and their interactions driven by the ponderomotive force of crossing laser beams.*, Proc. IFSA 2003, 213, 2003, and arXiv :1210.8105.

M. M., N. Crouseilles, E. Sonnendrücker, B. Afeyan, *High-order numerical methods for KEEN wave Vlasov-Poisson simulations,* Poster, PPPS, 16-21 june 2013, San Francisco.

M. M., C. Steiner, L. Marradi, N. Crouseilles, E. Sonnendrücker, B. Afeyan, *Vlasov on GPU (VOG project)*, ESAIM : Proc. Vol. 43, December 2013, CEMRACS 2012, 37–58.

C. Steiner, M. M., *A semi-Lagrangian discontinuous Galerkin scheme for Vlasov-Poisson equation*, Vlasovia 2013, poster session.

B. Afeyan, F. Casas, N. Crouseilles, A. Dodhy, E. Faou, M. M., E. Sonnendrücker, *Simulations of Kinetic Electrostatic Electron Nonlinear (KEEN) Waves with Two-Grid, Variable Velocity Resolution and High-Order Time-Splitting* hal-00977344, version 1